Microphysical and Near-Storm Environmental Control on the Maintenance of the 15 July 2015 MCS

Frederick Iat-Hin Tam, Ming-Jen Yang, Wen-Chau Lee
Department of Atmospheric Science, National Taiwan University, Taipei, Taiwan; National Center for Atmospheric Research, Boulder, Colorado

1. Introduction

- A case study on the 15 July 2015 nocturnal MCS **(Fig.1)** is used here to explore the possible nocturnal MCS maintenance in a **low-shear environment**.
- A robust **hydrometeor recirculation** (Siegel and Van den Heever 2013) process favors MCS maintenance by strengthening the mid-level updraft.
- Pre-MCS **low-level moisture distribution** is also important

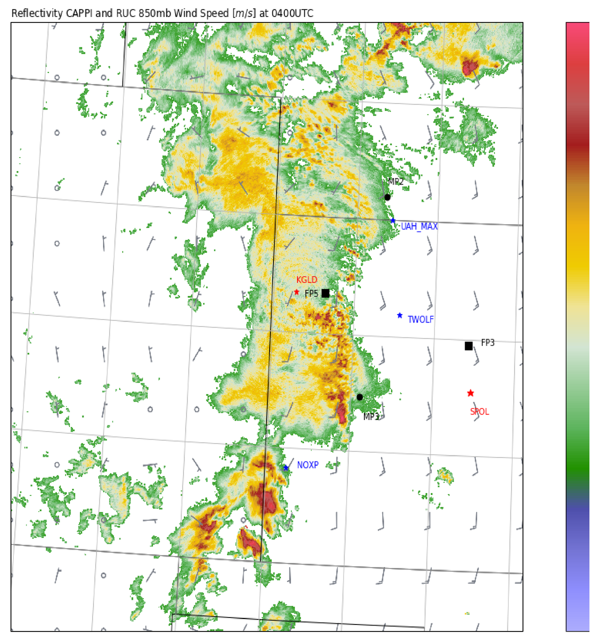

Fig.1 Reflectivity CAPPI and RAP 850mb wind (vector) at 0400UTC, 15 July 2015. The deployment location of PECAN mobile and fixed assets are also shown.

2. Methodology

- Pre-MCS environment sampling: High-frequency rawinsonde launches, surface observation and AERIoe thermodynamic profile retrieval data (Turner 2016) at FP5 (MCS_N) and MP2 (MCS_S), University of Wyoming King Air measurements.
- Dual-polarization level-II data from Goodland, Kansas and NOXP mobile radar data -> Non-meteorological signal filtering (Thresholds: ρ_{hv}>0.8, SW (Spectrum Width)<8.0)
- QC is performed with SOLO interactive editor (Oye et al. 1995). Processed data are plotted with the open-source Py-ART package (Helmus and Collis 2016).

3. Pre-MCS environment

3.1 Evolution of environmental instability

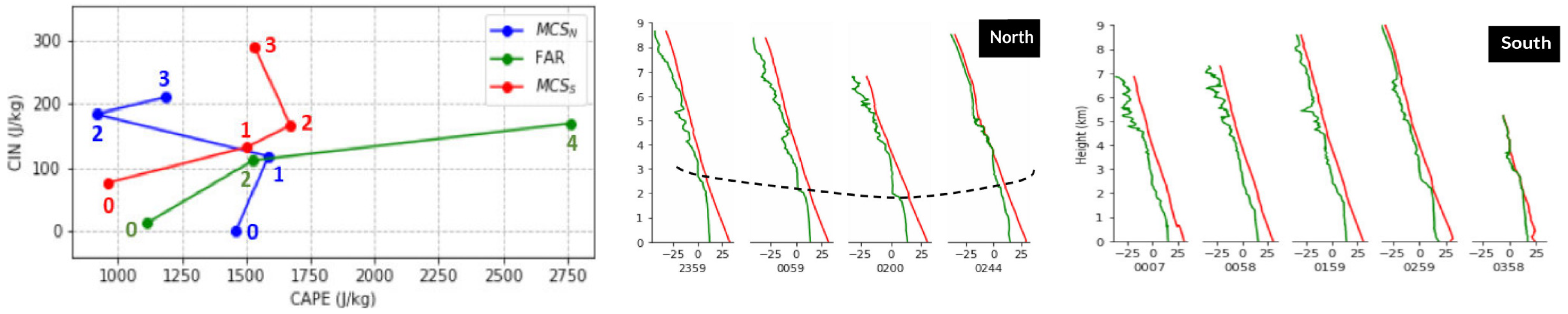

Fig.2 (a) MLCAPE-MLCIN evolution in pre-MCS_N <blue>, pre-MCS_S <red>, far environment <green> derived from sounding data. Numbers represent the approximate rawinsonde launch time. (b)(c) Temperature-Dewpoint profile in pre-MCS_N and pre-MCS_S environment

3.2 Difference in low-level moisture vertical distribution

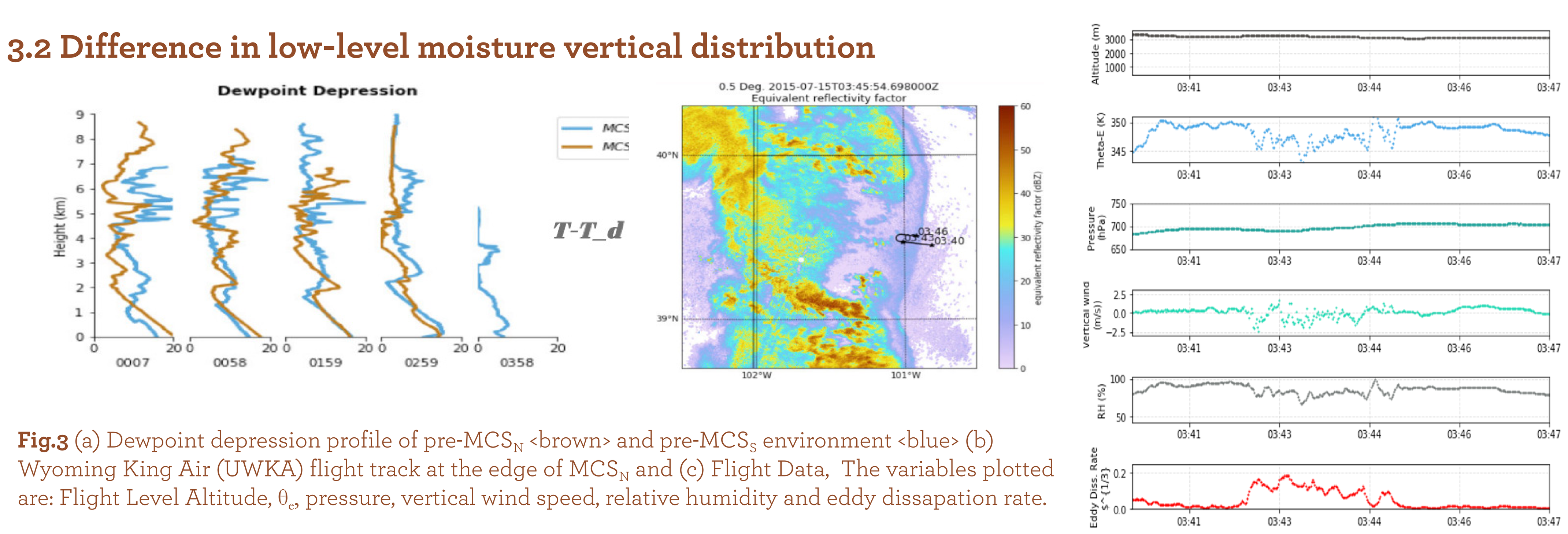

Fig.3 (a) Dewpoint depression profile of pre-MCS_N <brown> and pre-MCS_S environment <blue> (b) Wyoming King Air (UWKA) flight track at the edge of MCS_N and (c) Flight Data. The variables plotted are: Flight Level Altitude, θ_v, pressure, vertical wind speed, relative humidity and eddy dissapation rate.

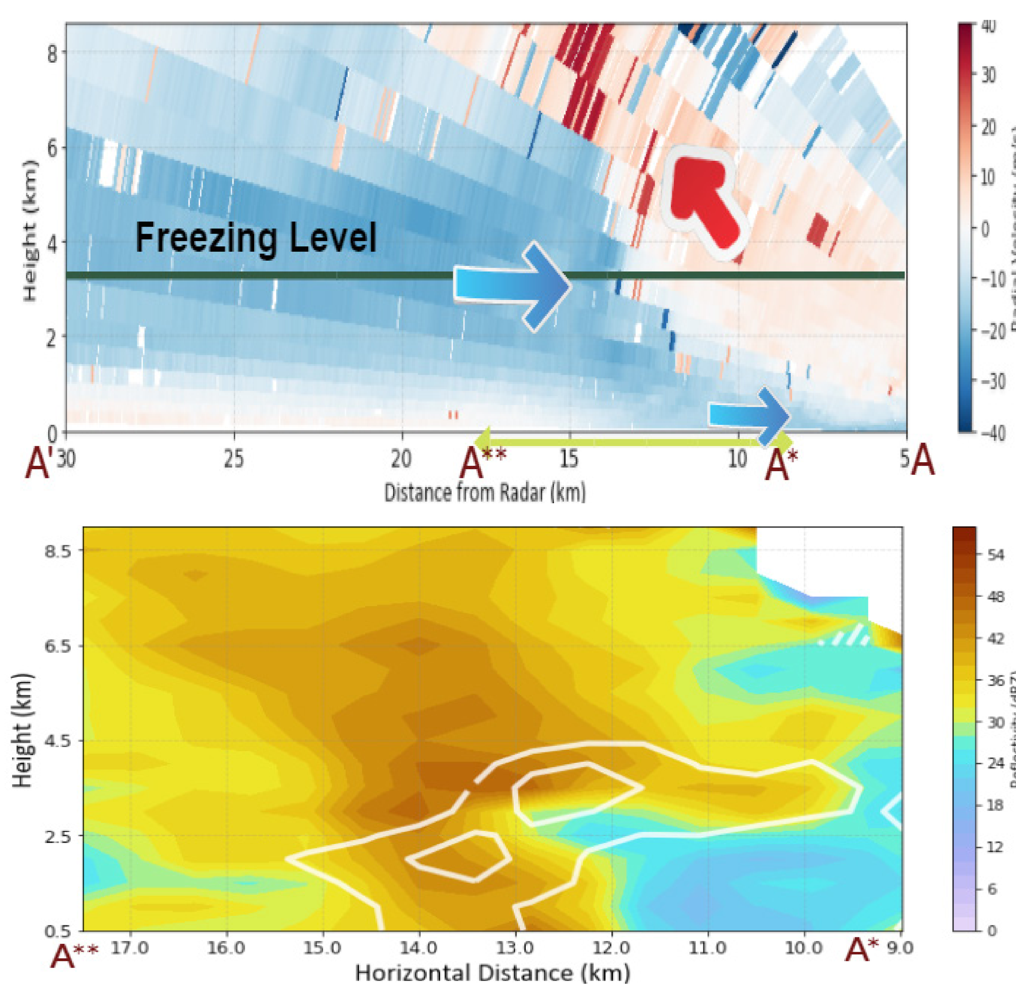

Fig.4 Radar observation of MCS_S along a 240° cross section at 0415UTC. (a) Radial Velocity, with approximate freezing level height marked.
(b) Reflectivity (Shading) and ZDR (contour) along the section with strongest inflow layer lifting

4. Microphysical structure

- NE-SW cross section (Fig.4a,b) through MCS_S shows strong inflow layer lifting. Rear inflow of MCS_S is strong and relatively deep, reaching ~30 m/s near MCS freezing level. **ZDR column** at the edge of strong convective cells (Fig.4b) is also indicative of a strong updraft.
- E-W cross section (Fig.5a,b) through MCS_N illustrates a lack of strong inflow layer lifting, weaker rear inflow , weaker and shallower reflectivity core.

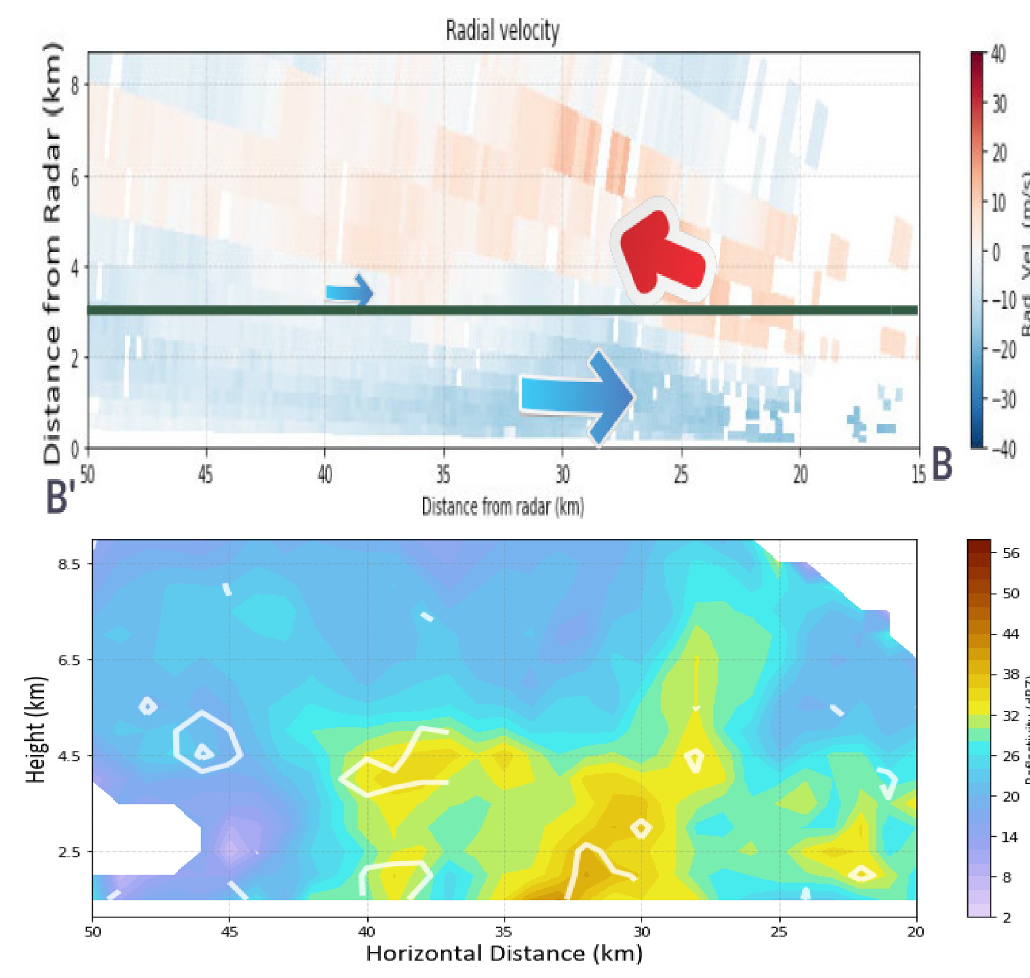

Fig.5 Radar observation of MCS_N along a 270° cross section at 0330UTC. (a) Radial Velocity, with approximate freezing level height marked.
(b) Reflectivity (Shading) and ZDR (contour) along the section with strongest inflow layer lifting

Eq.1a

$$V_q = \frac{\int_0^\infty V_x(D_x)m_x(D_x)N_x(D_x)dD_x}{\int_0^\infty m_x(D_x)N_x(D_x)dD_x} = \gamma a_x \frac{\Gamma(1+d_x+\alpha_x+b_x)}{\Gamma(1+d_x+\alpha_x)} \frac{\lambda_x^{1+d_x+\alpha_x}}{(\lambda_x+f_x)^{1+d_x+\alpha_x+b_x}}$$

Eq.1b

$$V_N = \frac{\int_0^\infty V_x(D_x)N_x(D_x)dD_x}{\int_0^\infty N_x(D_x)dD_x} = \gamma a_x \frac{\Gamma(1+\alpha_x+b_x)}{\Gamma(1+\alpha_x)} \frac{\lambda_x^{1+\alpha_x}}{(\lambda_x+f_x)^{1+\alpha_x+b_x}}$$

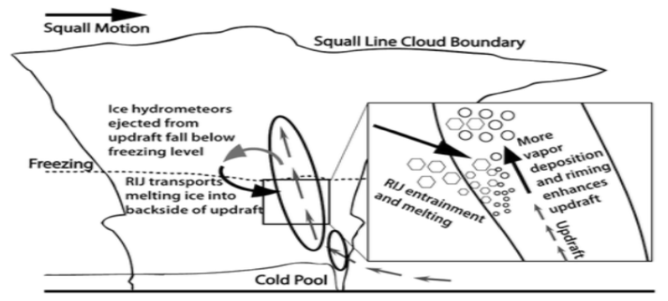

Domain	D1	D2	D3
Grid Size	27km	9km	3km
Vertical Levels	42	42	42
Cumulus	Kain-Fritsch	X	X
Microphysical	X	2M NSSL	2M NSSL
PBL	YSU	YSU	YSU

Fig.6 (a) Eq1a: Mass-weighted fall speed; Eq1b: Number-weighted fall speed (b) Schematic Diagram of Hydrometeor Recirculation Process (Siegel and Van den Heever 2013) (c) Model Setting

5. WRF simulation results

5.1 Experimental Design

- Two simulations are performed to test the microphysical sensitivity:

FULL (No change applied to 2M NSSL scheme)
GHNS (For graupel class, set mass-weighted fall speed (Eq.1a) for $N_{graupel}$)

5.2 MCS stuctural comparison

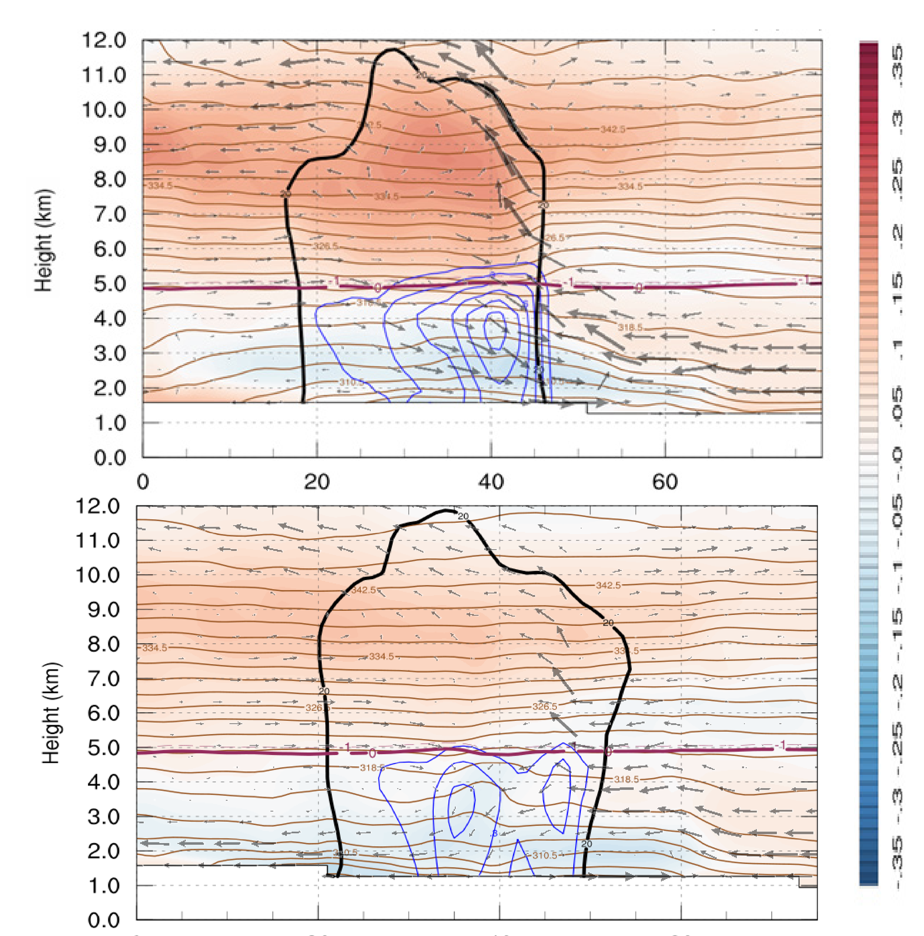

Fig.7 Line-averaged cross section of simulated (a) FULL (b) GHNS MCS (Shading: Buoyancy, Black Contour: 20dBZ, Blue contour: Rainwater mixing ratio, Vector: Line-Normal Wind)

5.3 CFAD Analysis

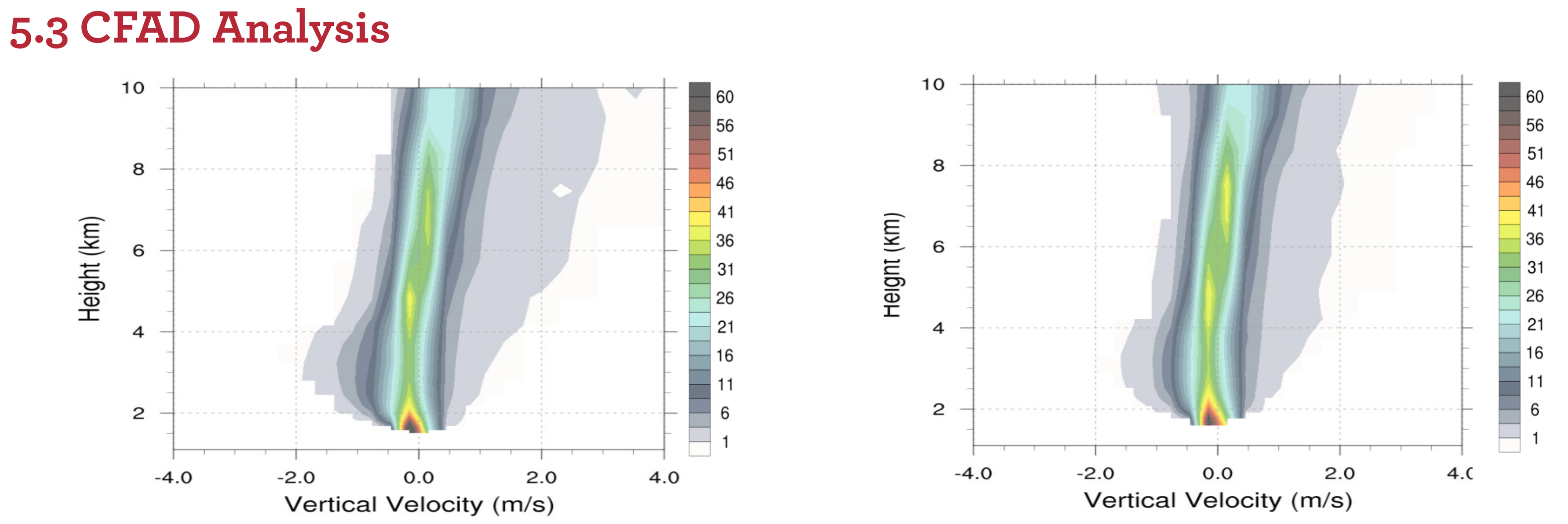

Fig.8 Vertical Velocity Contoured Frequency by Altitude Diagrams (CFADs) for (a) FULL (b) GHSS

6. Take-home

- **Strong rear inflow** -> Enhanced mid-level updraft -> Favorable for long-lived MCS
- 2M simulations indicate a sensitivity of recirculation process to **size-sorting**.
- Subtle changes in low-level moisture availability can be consequential

7. Acknowledgement

- This research is supported by the Ministry of Science and Technology of Taiwan under Grant MOST-106-2111-M-002-004
- The authors would like to thank Mr. J.E. Miao, Mr. Y.C. Wu, Ms. W.H. Chi for helpful discussions and suggestions. PECAN data are provided by NCAR/EOL.

國立臺灣大學 National Taiwan University
NCAR UCAR EOL Earth Observing Laboratory

Corresponding author:
Frederick Iat-Hin Tam, ft21894@gmail.com